ARMY RESEARCH LABORATORY

Pendeo-Epitaxy Process Optimization of GaN for Novel Devices Applications

by Michael A. Derenge, Tsvetanka S. Zheleva, Kenneth A. Jones, Pankaj B. Shah, Daniel Ewing, J. Molstad, Unchul Lee, Matthew H. Ervin, and David N. Stepp

ARL-TR-4426 **April 2008**

NOTICES

Disclaimers

The findings in this report are not to be construed as an official Department of the Army position unless so designated by other authorized documents.

Citation of manufacturer's or trade names does not constitute an official endorsement or approval of the use thereof.

Destroy this report when it is no longer needed. Do not return it to the originator.

Army Research Laboratory
Adelphi, MD 20783-1197

ARL-TR-4426 **April 2008**

Pendeo-Epitaxy Process Optimization of GaN for Novel Devices Applications

Michael A. Derenge, Tsvetanka S. Zheleva, Kenneth A. Jones, Pankaj B. Shah, Daniel Ewing, J. Molstad, Unchul Lee, Matthew H. Ervin, and David N. Stepp
Sensors and Electron Devices Directorate, ARL

REPORT DOCUMENTATION PAGE

Form Approved
OMB No. 0704-0188

1. REPORT DATE *(DD-MM-YYYY)*	2. REPORT TYPE	3. DATES COVERED (From - To)
April 2008		

4. TITLE AND SUBTITLE
Pendeo-Epitaxy Process Optimization of GaN for Novel Devices Applications

5a. CONTRACT NUMBER

5b. GRANT NUMBER

5c. PROGRAM ELEMENT NUMBER

6. AUTHOR(S)
Michael A. Derenge, Tsvetanka S. Zheleva, Kenneth A. Jones,
Pankaj B. Shah, Daniel Ewing, J. Molstad, Unchul Lee, Matthew H. Ervin,
and David N. Stepp

5d. PROJECT NUMBER

5e. TASK NUMBER

5f. WORK UNIT NUMBER

7. PERFORMING ORGANIZATION NAME(S) AND ADDRESS(ES)
U.S. Army Research Laboratory
ATTN: AMSRD-ARL-SE-RL
2800 Powder Mill Road
Adelphi, MD 20783-1197

8. PERFORMING ORGANIZATION REPORT NUMBER
ARL-TR-4426

9. SPONSORING/MONITORING AGENCY NAME(S) AND ADDRESS(ES)

10. SPONSOR/MONITOR'S ACRONYM(S)

11. SPONSOR/MONITOR'S REPORT NUMBER(S)

12. DISTRIBUTION/AVAILABILITY STATEMENT
Approved for public release; distribution unlimited.

13. SUPPLEMENTARY NOTES

14. ABSTRACT

A relatively new class of materials known as wide bandgap materials and the corresponding devices fabricated from them have extremely useful characteristics for high–temperature, high-frequency, high-power applications in numerous army systems and components. However the technology for these new materials is not mature enough and these materials contain various types of structural defects in high concentrations. It is well known that structural defects degrade the performance of the electronic devices and greatly diminish their reliability. Therefore various approaches for materials and devices optimization have been utilized in order to improve the operational characteristics of the wide bandgap electronic devices. One approach for defect reduction and improved electronic performance of wide-bandgap devices fabricated from material such as gallium nitride (GaN) is via pendeo-epitaxy. Pendeo-epitaxy as a technology is known to enable drastic reduction of the densities of structural defects in GaN over three to four orders of magnitude. We have used metal organic chemical vapor deposition (MOCVD) technique to grow pendeo-epitaxial (PE)-GaN, performed analysis of the morphology, structure, and electrical properties via numerous characterization techniques available at ARL, and correlated the materials and electrical characteristics with the growth and processing conditions. Further, we designed and fabricated test device structures in order to investigate the improved electronic performance of the Shottky contacts and high electron mobility transistors (HEMTs) and correlate the improved devices performance with the improved structural quality of the GaN material.

15. SUBJECT TERMS
Wide bandgap semiconductor devices, structure, defects, characterization, reliability, material device correlations

16. SECURITY CLASSIFICATION OF:			17. LIMITATION OF ABSTRACT	18. NUMBER OF PAGES	19a. NAME OF RESPONSIBLE PERSON
a. REPORT	b. ABSTRACT	c. THIS PAGE	SAR	22	Michael A. Derenge
Unclassified	Unclassified	Unclassified			19b. TELEPHONE NUMBER (*Include area code*) 301-394-1195

Standard Form 298 (Rev. 8/98)
Prescribed by ANSI Std. Z39.18

Contents

List of Figures iv

List of Tables iv

1. Introduction 1

2. MOCVD PE-GaN Growth Optimization 3

2.1 Results and Discussion 5

3. Characterization 7

3.1 Surface Microstructure 7

3.2 Structural Characterization 9

3.3 Optical Characterization: SEM-CL Correlation 11

4. PE-GaN Material for Novel RF Devices 11

5. Conclusions 13

6. References 14

Distribution List 15

List of Figures

Figure 1. (a) A schematic of the pendeo-epitaxial GaN approach. GaN grows vertically and laterally at the same time (b) Transmission electron microscopy (TEM) of pendeo-epitaxial GaN revealing two to four orders of magnitude lower density of dislocations in the regions of lateral growth (B) compared to the regions of vertical growth (A). 2

Figure 2. Reflectance recorded during standard MOCVD growth of underlying GaN on (0001) sapphire substrate. 4

Figure 3. Plan view SEM images of uncoalesced PE-GaN structures grown at different temperatures and crystallographic orientations of the stripes: along [11-20] (a-d) and along [1-100] (e-h). 5

Figure 4. Development of the top and side walls surface morphology and crystallography at different growth temperatures (a) 1060, (b) 1080, (c) 1100, and (d) 1120 ^{o}C. (e) A schematic of the side wall crystallography at different growth temperatures. 6

Figure 5. Variation of the vertical to lateral growth rate ratios at two different V:III ratios: (a) 1040 and (b) 2600. 7

Figure 6. PE-GaN growth progression in a 3x14 μm pattern at (a) 30 min, (b) 60 min, and (c) 90 min and pressure of 100 Torr and V:III ratio of 2600. 7

Figure 7. (a) SEM image from the top (0001) surface of the PE-GaN stripes in 2x14 μm pattern. (b) AFM micrograph acquired from the (0001) GaN stripe area. 8

Figure 8. Etch pit distribution in the (a) PE-GaN stripe in 2x20 μm pattern and (b) conventional GaN layer grown simultaneously at the near vicinity of the striped PE-GaN. The bar in the SEM image is 4 μm. 9

Figure 9. (a) Selected area diffraction pattern, (b) cross-sectional TEM, (c) a schematic of an open core screw dislocation and (d) plan view HRTEM from an open core screw dislocation in PE-GaN heterostraucture. 10

Figure 10. SEM and the corresponding CL image in plan view (a, b) and cross-section (c, d) from PE-GaN structure in 2x14 μm pattern. Note that in the CL images (b) and (d) the seed/column regions associated with high density of dislocations appear dark and in contrast, the regions of lateral PE-GaN growth appear bright. 12

Figure 11. PE-GaN HEMT mask designed to position the gates over the low defect density PE-GaN regions to test the device performance and reliability. 12

List of Tables

Table 1. Properties of GaN compared to other materials. 1

1. Introduction

Our objective is to develop advanced RF components for high performance surveillance and target acquisition radar systems and pursue technologies that will enable smaller, lighter, more efficient and affordable electronically scanning antennas and communications for future army systems. In this respect wide bandgap materials (such as GaN, AlN, InN) and the devices, components and systems built from them offer a vast potential for increased performance and reliability compared to the conventional Si and GaAs materials and devices (Yoder, 1996; Kemerley et al., 2002).

Gallium nitride (GaN) and related materials (such as AlN and their alloys), are next generation wide bandgap materials that are promising for advanced electronic and optoelectronic applications. For example, the wide band-gap of GaN, its high saturation drift velocity, and high electron mobility make it very useful for high temperature, high frequency, high power devices that can be used in harsh environments. In addition, the capacity of the GaN-based materials to alloy with aluminum and indium allows it to cover a broad spectral range that makes it exceptional for optoelectronic applications, such as light emitting diodes, laser diodes, and UV detectors. Also, the existence of the AlGaN/GaN heterostructure allows the formation of a two dimensional electron gas (2DEG) and the formation of piezoelectronically induced sheet carriers. The piezoelectric effect is over three times stronger in GaN compared to GaAs and contributes to the high sheet electron densities in AlGaN/GaN high electron mobility transistors (HEMTs). These advantages are evident when one calculates the combined figure of merit (CFOM) to compare device performance at high frequencies and at high powers based on individual material parameters (table 1) (Chow, T. P., 1994).

Table 1. Properties of GaN compared to other materials.

Material	Unit	Si	GaAs	4H-SiC	GaN
Bandgap Energy (Eg)	eV	1.12	1.42	3.26	3.41
Dielectric Constant (ε_r)		11.8	12.8	9.6	8.9
Thermal Conductivity (k_{th})	W/mK	150	50	380	170
Dielectric Breakdown (E_b)	V/cm	$4x10^6$	$5x10^5$	$2.2x10^6$	$5x10^6$
Saturation velocity (v_s)	cm/s	$1x10^7$	$2x10^7$	$2.0x10^7$	$3x10^7$
Electron Mobility (μ_e)	cm^2/Vs	1350	8500	1140	1500
CFOM		**1**	**8**	**404**	**489**

$$CFOM = E_g k_{th} \varepsilon_\rho \mu \nu_s E_B^{\,2} / (E_g k_{th} \varepsilon_\rho \mu \nu_s E_B^{\,2})_{silicon}$$

However, many of the useful characteristics of GaN cannot be applied to their full potential due to the high density of structural defects (in the order of 10^9 cm^{-2}). Due to the lack of wafer size native substrate that would provide the mechanisms for low defect density homoepitaxial growth of layers of GaN, other foreign substrates, mainly sapphire, SiC and recently silicon have been used implementing heteroepitaxial growth mechanisims. Homoepitaxy is the growth on native substrate (crystal) of the same material (GaN on GaN) while heteroepitaxy is the growth on a foreign substrate of a different materials (GaN on Si, sapphire, AlN or SiC). Heteroepitaxy growth mechanism are associated with large lattice and thermal mismatch at the hetero-interfaces resulting in structural defects such as dislocations, stacking faults and grain boundaries, that degrade the performance of the electronic and optoelectronic devices.

Therefore, new approaches for GaN heteroepitaxy were developed in recent years: the lateral epitaxial overgrowth (LEO) and the pendeo-epitaxy (PE) approaches known under the common name selective area epitaxy (SAE) (Nam et al., 1998; Zheleva et al., 2001; Davis et al., 2002; Fini P. et al., 2000; Coltrin et al., 1999). For example, the GaN films grown via a metal-organic chemical vapor deposition (MOCVD) technique using pendeo-epitaxy can have two to four orders of magnitude lower density of defects, compared to the conventional heteroepitaxy technique (figure 1).

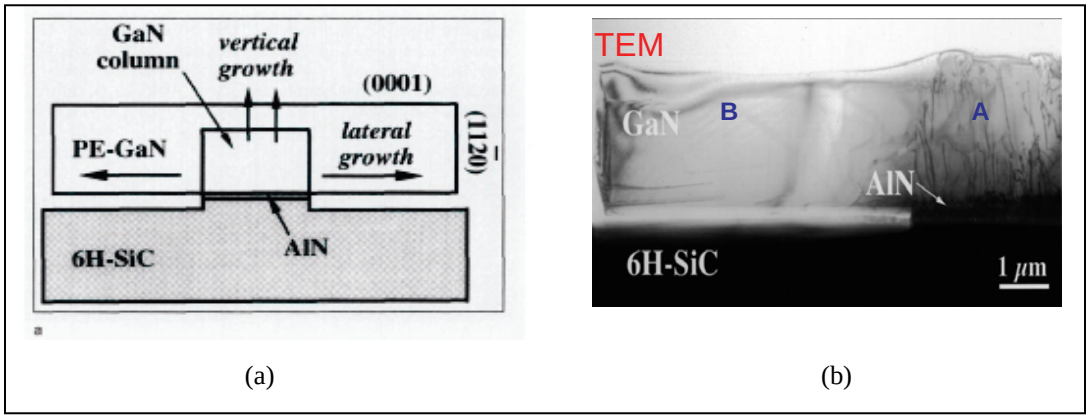

Figure 1. (a) A schematic of the pendeo-epitaxial GaN approach. GaN grows vertically and laterally at the same time (b) Transmission electron microscopy (TEM) of pendeo-epitaxial GaN revealing two to four orders of magnitude lower density of dislocations in the regions of lateral growth (B) compared to the regions of vertical growth (A).

Pendeo-epitaxial technology for growth of GaN uses the lateral epitaxial growth mechanisms to enable the GaN material to grow nearly defect free laterally from the side walls of etched GaN rectangular columns. The pendeo-epitaxial growth process involves the following three major steps: (i) MOCVD growth of continuous underlying GaN film, 1.5 - 3 μm thick, on sapphire, SiC, or Si substrate; (ii) etching of rectangular columns/trenches in the underlying GaN using standard photo lithography technique and dry etching in ICP-RIE; and (iii) regrowth of low defect density GaN from the side walls and top surfaces of the etch columns. Given substantially

long growth time, two adjacent growth fronts meet and coalesce, followed by a continuous GaN film growth. It is our goal to use the low defect density regions of the lateral PE-GaN to position the active gate regions of GaN HEMT devices in order to explore the role of defects on the HEMTs performance by comparing it to the HEMTs grown on conventional GaN.

Our approach includes the following steps: (i) MOCVD PE-GaN growth optimization; (ii) processing optimization; (iii) characterization of the surface morphology of PE-GaN via scanning electron microscopy (SEM), profilometry, atomic force microscopy (AFM), etch pit density (EPD); characterization of the optical properties via cathodoluminescence (CL), photoluminescence (PL), and Raman spectroscopy. The structural properties of the PE-GaN were characterized via x-ray diffraction (XRD) and transmission electron microscopy (TEM). The electrical characteristics of the underlying GaN and the PE-GaN were studied via four point probe and Hall techniques.

2. MOCVD PE-GaN Growth Optimization

The most widely used approach for growth of high quality GaN layers via pendeo-epitaxy uses the metal organic chemical vapor deposition (MOCVD) technique that commonly requires ammonia (NH_3) and trimethyl gallium (TMG) as precursors, high partial pressure of ammonia (NH_3), high growth temperatures; and also a low temperature nucleation layer to accommodate the mismatch. The various stages of the MOCVD growth of GaN are monitored via the in-situ reflectance interferometry (RI) technique. Reflectance interferometry analyses of the GaN epitaxial layer having a different refractive index from the sapphire substrate. Thus, the reflected light intensity follows a periodic function, with a period that is proportional to the wavelength of the incident light and cosine of the angle of incidence, and inversely proportional to the refractive index of the epilayer at the growth temperature and the growth rate. When the light is absorbed or scattered by roughening of the surface, the oscillations are damped. Inversely, smooth shiny surface gives strong periodic oscillations. A typical recording of the reflectance signal during the epitaxial growth of GaN on sapphire is shown in figure 2.

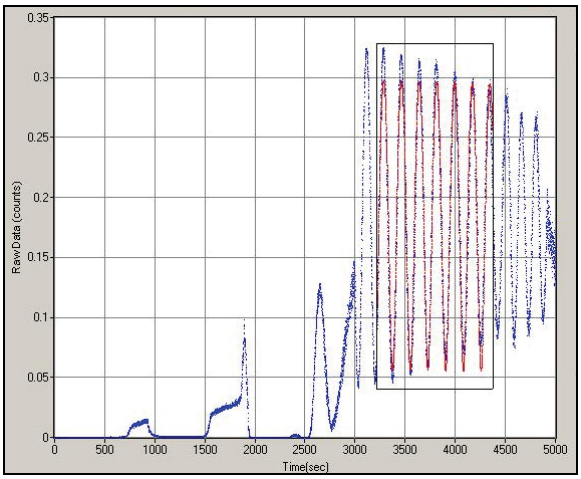

Figure 2. Reflectance recorded during standard MOCVD growth of underlying GaN on (0001) sapphire substrate.

The low temperature GaN or AlGaN nucleation layer, the underlying GaN seed layer and the PE-GaN and AlGaN layer were grown sequentially on a sapphire (0001) substrate in a cold-wall, vertical MOCVD system. The 0.03 μm thick low temperature GaN nucleation layer and the 0.5 μm thick GaN seed layers are grown at 400 Torr and temperatures of 580 ^{o}C and 1100 ^{o}C, respectively. A 1 μm layer was deposited at 100 Torr and 111 ^{o}C to smooth the rough nucleation layer. Cr and Ni layers of 30 nm and 400 nm thickness, respectively are deposited on patterned photoresist stripes on each GaN seed layer by e-beam evaporation. Standard "lift-off technique", using acetone and ultrasonic agitation, was used to pattern the Ni etch mask. The unmasked striped regions were etched off through the GaN thickness and into the sapphire in an inductively coupled plasma reactive ion etching system (ICP) in a mixture of Cl_2 and BCl_3 gases. Subsequently the Cr/Ni layers were removed using 4 minute dip in Nickel etch (HNO3:CH3COOH:H2SO4:water with proportions5:5:2:15) solution, then one minute in CR-9 (CYANTEK CORPORATION) Chrome etch. The remaining GaN seed layer consisted of 2, 3, 4, and 5 μm stripes oriented along the [1-100] and/or [11-20] directions, separated by distances of 8, 7, 6, and 5 μm, respectively. In another mask setting, the GaN seed layer consisted of 2 and 3 μm wide stripes, separated by distances of 12, 14, and 20 μm.

Major MOCVD growth parameters that are known to influence the lateral growth rate and the crystallography of the side walls of the pendeo-epitaxial GaN are the growth temperature, the ammonia to TMG flow rate ratio (V:III ratio), the chamber pressure and the time to coalescence (Nam et al., 1998; Zheleva et al., 2001; Roskowski et al., 2002). We have varied each of these parameters while keeping the rest constant in order to investigate the role that each of them plays for enhanced lateral growth, surface microstructure, defect density distribution, structural, optical and electrical characteristics of the GaN and AlGaN layers related to the HEMT device structures.

2.1 Results and Discussion

The effects of the growth temperature and the stripe orientation on the PE-GaN lateral growth rate and the side wall morphology and crystallography are shown in figure 3. The growth temperature was varied by 20 ^{o}C increments from 1060 ^{o}C to 1120 ^{o}C. These images reveal that the PE-GaN growth for the stripes along [11-20] direction proceed by formation of the inclined (11-22) side facets, with very narrow top (0001) surfaces. The growth along the [1-100] direction of the GaN seed stripes proceeds by formation of the flat and very smooth top (0001) surfaces and the formation of the vertical (11-20) walls. The presence of these vertical side walls is essential for the coherent coalescence of the adjacent Pe-GaN wings and the subsequent smooth continuous GaN film growth.

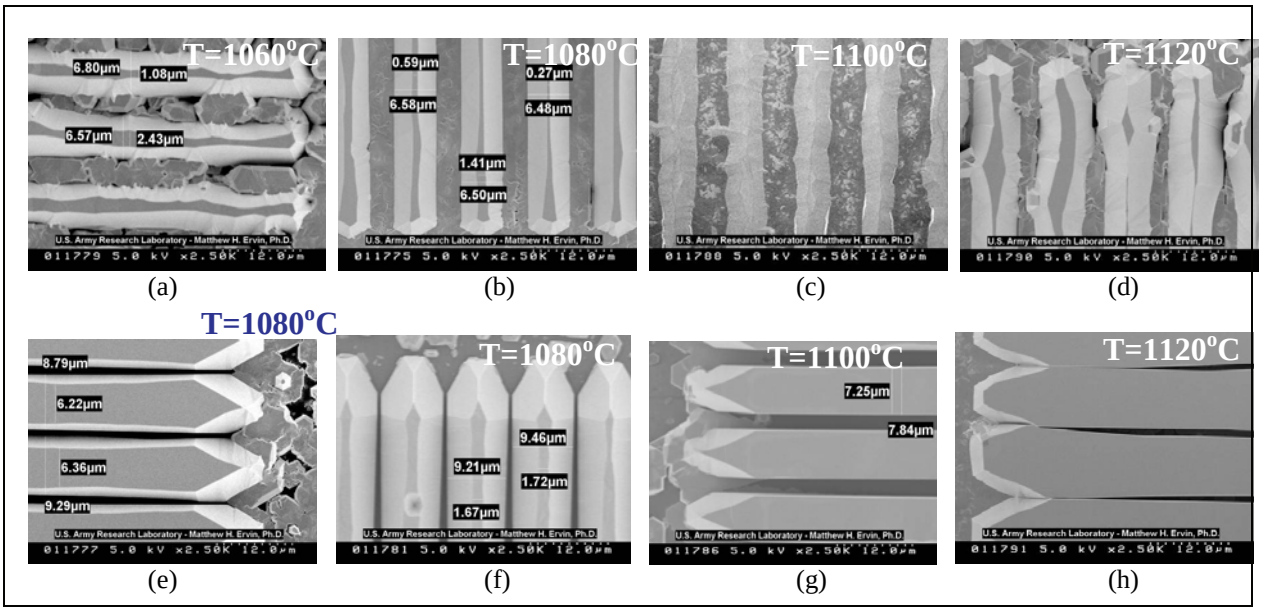

Figure 3. Plan view SEM images of uncoalesced PE-GaN structures grown at different temperatures and crystallographic orientations of the stripes: along [11-20] (a-d) and along [1-100] (e-h).

The PE-GaN stripes 4 µm wide and spaced at 6 µm are shown in the SEM micrographs in figure 4(a-d) and schematically in figure 4(e). As in the conventional LEO case (Zheleva, 2001), the PE-GaN structure exhibits a tendency for increase of the lateral growth rate. The morphologies of the PE-GaN grown along the [1-100] seed GaN stripe direction at different temperatures grow with increased lateral growth rate and at the same time reduced vertical growth rate, when the growth temperature increases from 1060 ^{o}C to 1120 ^{o}C. Concurrently the side wall crystallography changes from exhibiting the (11-22) and (11-20) planes at 1060 ^{o}C, thus forming trapezoidal cross-section (figure 4(a) to being the vertical (11-20) planes at temperatures higher than 1080 ^{o}C. As the growth temperature increases, the width of the top (0001) faces increases until the elimination of the slanted (11-22) walls. Only the vertical (1-100) side walls present at 1080 ^{o}C and higher temperatures.

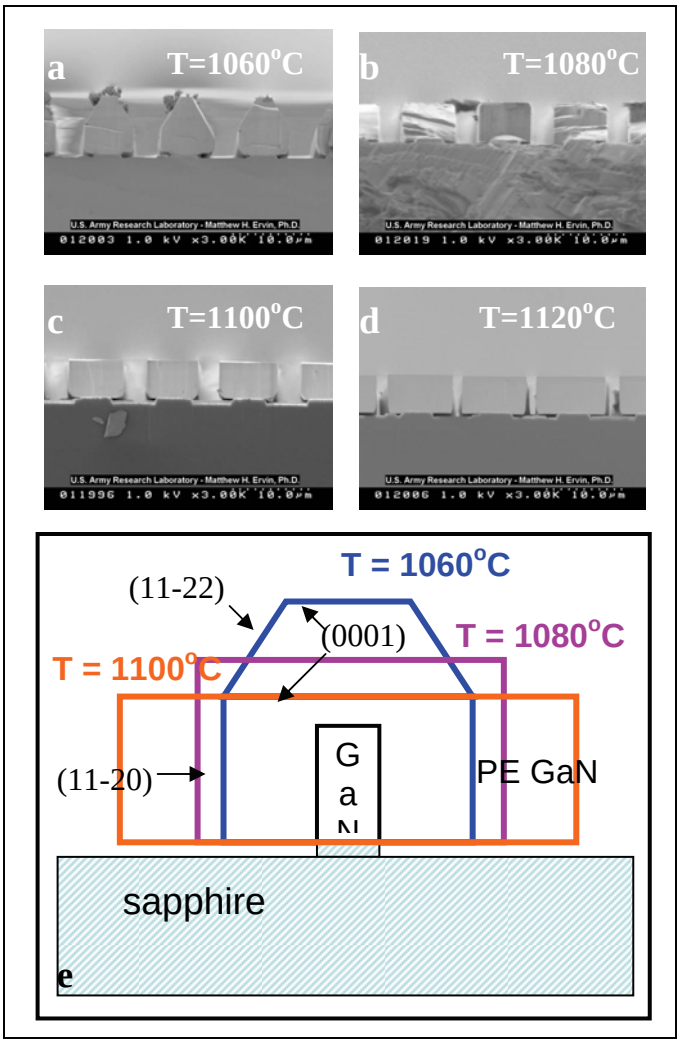

Figure 4. Development of the top and side walls surface morphology and crystallography at different growth temperatures (a) 1060, (b) 1080, (c) 1100, and (d) 1120 °C. (e) A schematic of the side wall crystallography at different growth temperatures.

It is known that the ammonia to TMG (V:III) molar flow rate ratio plays a major role for the lateral to vertical growth rate ratio. Increase of the V:III ratio leads to increase of the lateral to the vertical growth rate ratio, as shown in figure 5. Another step in the MOCVD optimization process was the achievement of continuous and smooth PE-GaN and AlGaN layers after the coalescence of the side walls. Cross-sectional SEM images of the PE-GaN structures as a function of the growth time before and after the coalescence revealing smooth top (0001) GaN surfaces and typical voids at the coalesced fronts, associated with the non-uniformity of the side walls development as the lateral growth front meet due to change in the incoming gas fluxes and the incorporation of the adatoms to the side planes are shown in figure 6.

Thus, the optimized growth conditions for the PE-GaN were achieved at high growth temperatures above 1100 ^{o}C, high V:III ratio of 2600, and at 100 Torr chamber pressure. At the vertical growth rate of 2.5 μm /hr after 60 minutes of growth the lateral growth fronts coalesce for 3x14 μm pattern, thus achieving 7 μm/hr lateral growth rate and smooth continuous GaN layer.

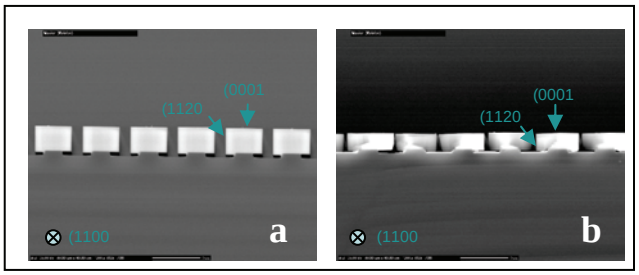

Figure 5. Variation of the vertical to lateral growth rate ratios at two different V:III ratios: (a) 1040 and (b) 2600.

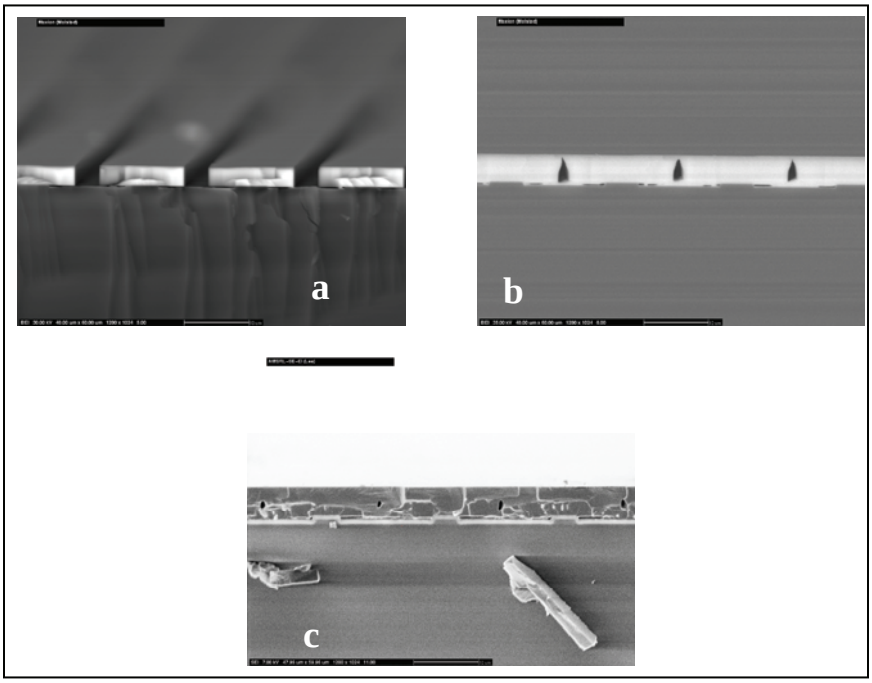

Figure 6. PE-GaN growth progression in a 3x14 μm pattern at (a) 30 min, (b) 60 min, and (c) 90 min and pressure of 100 Torr and V:III ratio of 2600.

3. Characterization

3.1 Surface Microstructure

The surface morphology of the PE-GaN was characterized via SEM and AFM. Plan view SEM images reveal very smooth top surfaces of the regrown PE-GaN as shown in figure 7. It is

notable that the formation of hillocks in the center of PE-GaN column observed both via SEM and AFM, figure 7 (a) and (b), respectively.

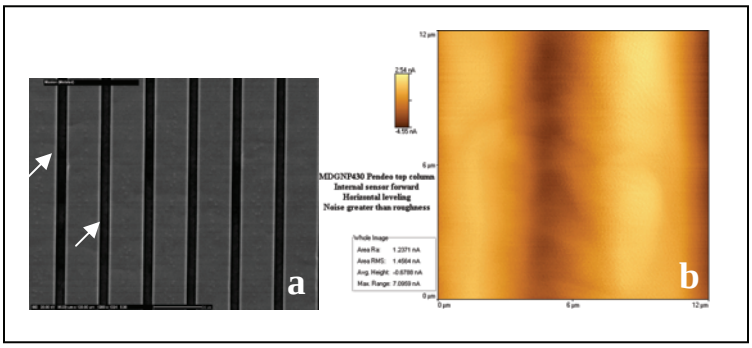

Figure 7. (a) SEM image from the top (0001) surface of the PE-GaN stripes in 2x14 μm pattern. (b) AFM micrograph acquired from the (0001) GaN stripe area.

It is determined that the hillocks are associated with growth instabilities and are a consequence of preferential growth at heterogeneous steps, originating at the intersection of threading dislocations with screw and edge character and the (0001) growth surface. It is evident that the hillocks are distributed only at the central column regions of PE-GaN stripe that is associated with the vertical growth and the corresponding higher density of threading dislocations that are related to the conventional growth mechanisms.

When the sample is dipped in a molten KOH at 480 ^{o}C, etch pits are formed on the surface, commonly with hexagonal shape, observed via SEM at the central regions, as shown in figure 8. This is additional support of the statement that the hillocks at the center of the PE-GaN columns are associated with the threading dislocations. As one can see from figure 8 (a) these etch pits are distributed only at the center of the PE-GaN columns and are associated with the threading dislocations that propagate from the underlying seed GaN/sapphire interface up to the top surface. One can estimate the etch pit density (EPD) at these central regions to be in the order of low 10^{9} cm^{-2}. Away from the central regions the surface is nearly etch-pit free. This is, in essence, the effect of the lateral growth mechanisms associated with the pendeo-epitaxial process. In contrast, the uniform distribution of the EPD associated with the conventional GaN growth is shown in figure 8 (b).

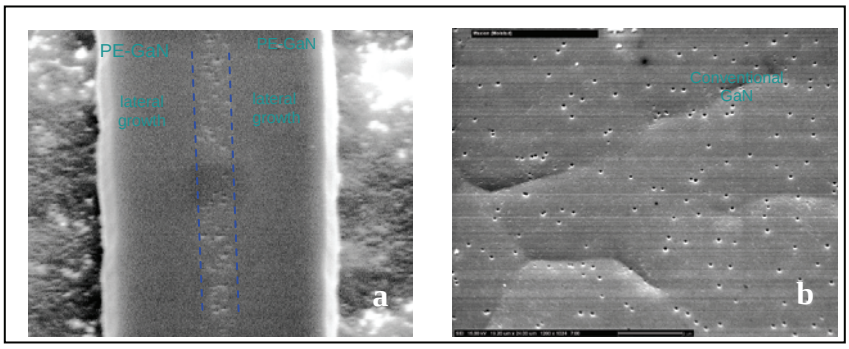

Figure 8. Etch pit distribution in the (a) PE-GaN stripe in 2x20 μm pattern and (b) conventional GaN layer grown simultaneously at the near vicinity of the striped PE-GaN. The bar in the SEM image is 4 μm.

3.2 Structural Characterization

TEM images in cross-sectional and plan-view reveal the microstructure of the PE-GaN material, the quality of the film-substrate interface, the presence and distribution of structural defects. The PE-GaN layer is a single crystal, as revealed from the selected area diffraction pattern in figure 9(a). However, the high density of threading, edge, screw and mixed character dislocations in the order of low 10^9 cm^{-2}, that appear as dark lines, is typical for the regions corresponding to the conventional vertical growth of GaN [region "A" in figure 9(b)]. The regions of the pendeo-epitaxial growth [region "B" in figure 9(b)] exhibit two-to-four orders of magnitude lower dislocations density. It is important to note that most of the dark wavy lines in the PE-GaN (region B) are bend contours, related to the bending of the thin TEM foil and not associated with structural defects as threading dislocations or stacking faults. In addition, it is typical to observe the 90^o bending of the threading dislocations at the transition from the vertical to the lateral growth, as pointed by the white arrow in figure 9(b). Plan view TEM images reveal similar distribution of high density of threading dislocations in the regions of vertical growth and nearly defect-free regions corresponding to the PE-GaN. A schematic and high resolution plan-view TEM image of a threading screw dislocation are shown in figure 9(c) and (d), respectively.

Generally, there are two mechanisms that explain the reduction of the threading dislocation density associated with the lateral epitaxy phenomenon: the first one is derived from the "image force" approach and the other is the energy minimization approach. The "image force" approach derives its explanation from the understanding that a dislocation generates a stress field that has to be compensated when a dislocation gets close to a free surface. A virtual image dislocation is placed outside of the crystal and generates a stress field compensating the stress field of the actual dislocation. Such image dislocation exerts an attractive image force acting on the inner dislocation. During the conventional GaN epitaxial growth, a threading dislocation in the planar (0001) GaN film propagates along the [0001] direction because it is attracted only by the image force produced by the top (0001) facet. During the selected area growth (SAG, LEO and/or PE) of GaN, the growth is such that the stripes are defined by two side facets of (11-20) type and one top facet (0001). The {1120} planes form a 90^o angle with the (0001) plane. Thus, there are two

competing image forces acting on the dislocation in SAG that attract the dislocation toward the top surface and toward the side facets: When the lateral image force becomes greater than the vertical one, the dislocation bends from the vertical direction of propagation. Another explanation for the reduced density of structural defects during the SAG is the minimum energy consideration. According to this principle, for a given crystal the energy of a dislocation depends on its Burgers vector b and its line direction, and the dislocation propagates along the direction that minimizes its energy E(φ) :

$$E(\varphi) = 1/4p \,.\, b^2 \,.\, K(\varphi) \,.\, \ln R/r,$$

where φ is the angle between the dislocation line and it's Burger's vector b, K(φ) is an angular energy factor, and R, r are the outer and inner radii of the elastic field around the dislocation.

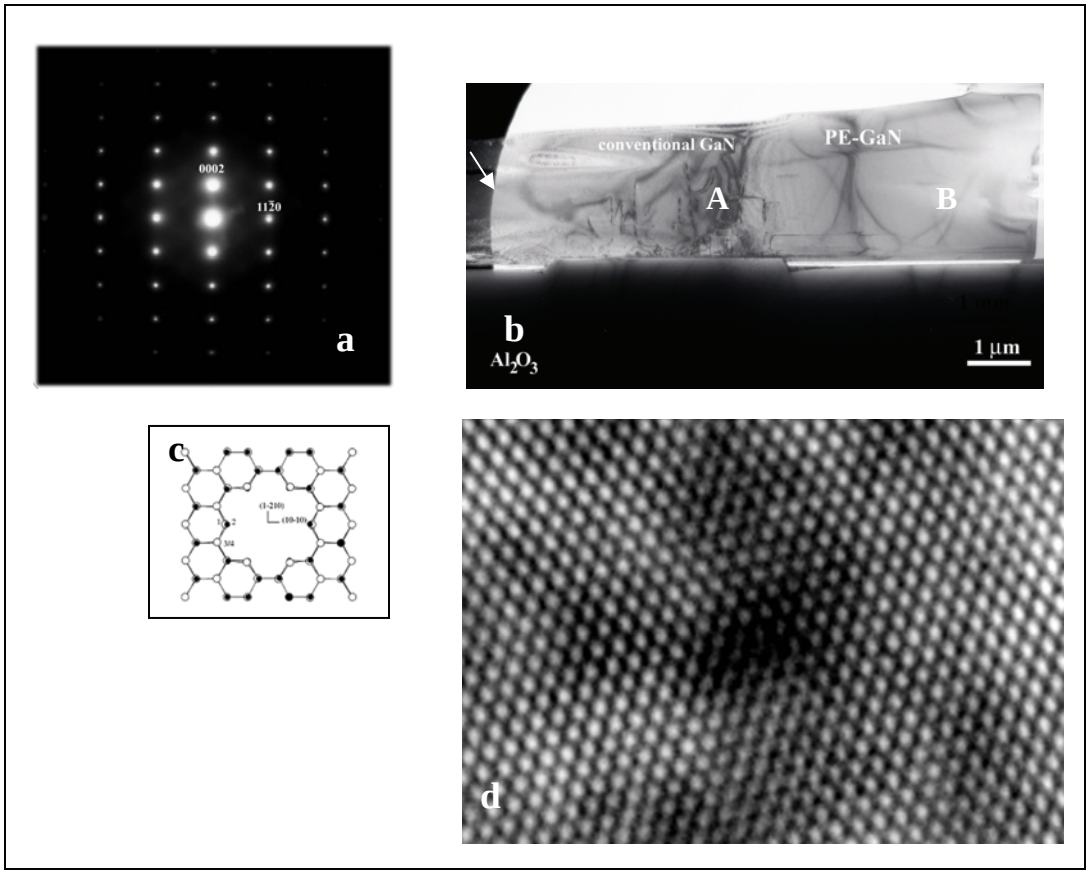

Figure 9. (a) Selected area diffraction pattern, (b) cross-sectional TEM, (c) a schematic of an open core screw dislocation and (d) plan view HRTEM from an open core screw dislocation in PE-GaN heterostraucture.

In addition, the minimum energy is achieved when the dislocation has a pure screw character (Stadelman, 2004).

Studies indicate that the distribution of the defects in the TEM images correlate well with the EPD distribution observed in the SEM images and also the CL images, as will be pointed out in the next section.

3.3 Optical Characterization: SEM-CL Correlation

Preliminary comparative studies with SEM and CL spectroscopy taken from the identical regions were performed to obtain information about the uniformity of the structural/optical quality of the PE-GaN material in the column/seed regions of vertuical growth and the PE-GaN regions of lateral growth. Figure 10 shows the SEM and the corresponding CL images in a plan-view (figure 10(a,b)) and in a cross-sectional-view (figure 10(c,d)). As one can see the central/column regions associated with the vertical growth that exhibit large density of dislocations as revealed by EPD calculations and TEM studies, appear dark in the CL images both in cross-section and plan-view. In contrast, the regions of lateral PE-GaN growth, known to have few orders of magnitude lower density of structural defects, appear bright. The change of growth front direction appears to influence not only the dislocation distribution but also the distribution of the emission properties (Paskova, 2002). Detailed analysis of the correlation between the dominating dislocation and point defect type, and the dominant emission mechanism is needed to fully understand PE-GaN material properties and the associated growth mechanisms responsible for them.

4. PE-GaN Material for Novel RF Devices

It is known that the higher structural quality of the epitaxial heterostructures results in devices that have superior electrical and electronic characteristics and thus improved reliability. The effect of the GaN structural quality on the electrical characteristics of p-n junctions has been studied using LEO-GaN material through current – voltage measurements (Kozodoy, 1998). A comparison of p-n diodes fabricated on the high defect density window region and the low defect density region of lateral overgrowth results in reduction of the reverse-bias leakage current by three orders of magnitude in the low defect density regions. Thus, it is expected that the improved structural quality of the PE-GaN material will result in improved leakage current of Shottky diodes, as well as improved mobility, power output, and power added efficiency of HEMTS fabricated on the PE-GaN. We designed series of masks in order to explore the advantages that the improved structural quality of the PE-GaN material will bring to the electrical performance of the HEMTs, as shown in figure 11. Preliminary studies on the Shottky contacts fabricated on the low defect density PE-GaN regions exhibit over an order of magnitude lower leakage currents compared to Shottky contacts fabricated on the conventional GaN.

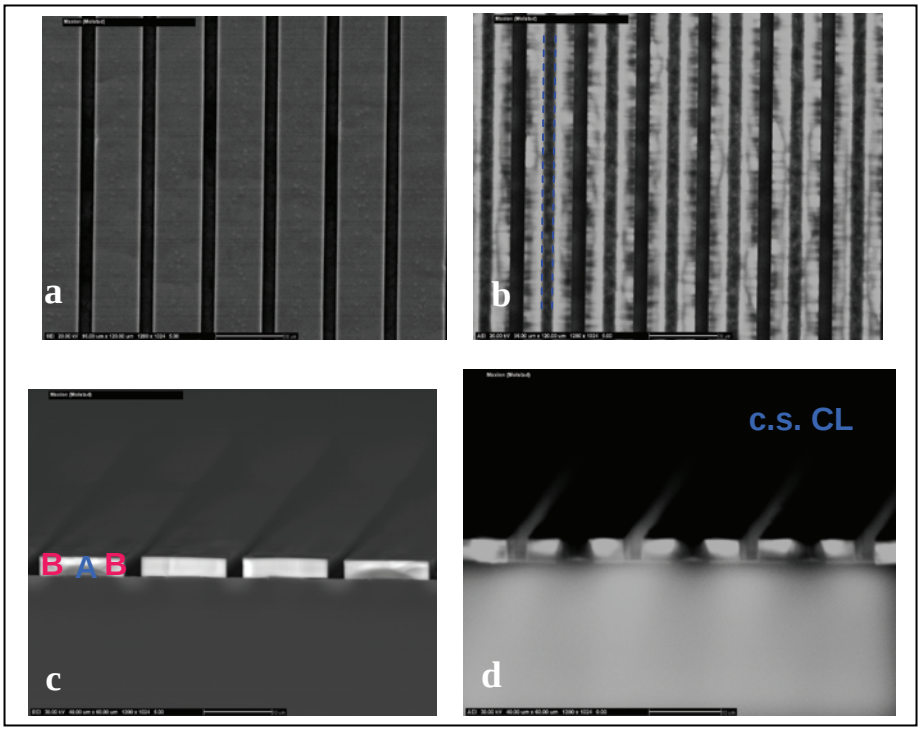

Figure 10. SEM and the corresponding CL image in plan view (a, b) and cross-section (c, d) from PE-GaN structure in 2x14 μm pattern. Note that in the CL images (b) and (d) the seed/column regions associated with high density of dislocations appear dark and in contrast, the regions of lateral PE-GaN growth appear bright.

We have initiated series of collaborative efforts in order to understand how the improved material quality of the PE-GaN correlates with the superior performance of the PE-GaN HEMTs and to identify the mechanisms by which structural defects influence the electrical characteristics of the devices. Also, we plan to use the PE-GaN material as a test system for reliability studies of the RF electronic devices and to correlate the improvement in the devices mobility, gain, PAE, lifetime and other critical parameters.

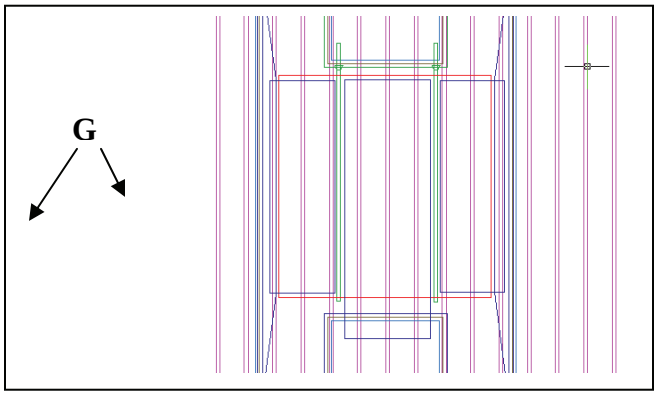

Figure 11. PE-GaN HEMT mask designed to position the gates over the low defect density PE-GaN regions to test the device performance and reliability.

5. Conclusions

Optimization of the MOCVD process has been conducted in order to achieve controllable and reproducible pendeo-epitaxial GaN material of superior structural quality, having two-to-four orders of magnitude lower density of dislocations. The MOCVD growth factors that enhance the lateral growth rate are the high growth temperature, 1100-1120 ^{o}C, the high V:III ratio of 2600; after 60 minutes of growth the lateral growth fronts coalesce (ex. for 3x14 μm pattern), achieving smooth and flat film with RMS roughness of 1.4 nm. Dislocation density is drastically reduced via the pendeo-epitaxial growth mechanisms from being 2.10^{9} cm^{-2} to less than 10^{6} cm^{-2}.

The material of improved structural quality and WBG devices of superior characteristics fabricated from this material will enable improved RF amplifier component capabilities that greatly improve the radar, communications and other DoD systems architectures.

6. References

Coltrin, M.; Willan, C.; Bartram, M.; Han, J.; Missert, N.; Crawfort, M.; Baca, A. Transport, Growth Mechanisms, and Material Quality in GaN Epitaxial lateral Overgrowth. *MRS Internet J. Nitride Semicond. Res.* **1999**, *4S1*, G6.9.

Chow, T. Paul; Tyagi, Ritu. *IEEE Transactions on Electron Devices* **1994**, *41* (8), 1481.

Davis, R. F.; Gehrke, T.; Linthicum, K.; Zheleva, T. S.; Rajagopal, P.; Zorman, C.; Mehregany, M. Pendeo-Epitaxial Growth and Characterization of Thin Films of Gallium Nitride and Related materials on SiC(0001) and Si(111) Substrates. *Z. Metallkunde* **2001**, *92*, 163–166.

Fini, P.; Marchand, H.; Ibbetson, J. P. Determination of Tilt in the Lateral Epitaxial Overgrowth of GaN using S-ray Diffraction. *Journal of Crystal Growth* **2000**, *209* (4), 581–590.

Kemerley, R.; Wallace, H. B.; Yoder, M. Impact of Wide Bandgap Microwave Devices on DoD Systems. *In Proceedings of the IEEE* **2002**, *90*, 1059–1064.

Kozodoy, P.; Ibbetson, J. P.; Marchand, H.; Fini, P. T.; Keller, S.; Speck, J. S.; DenBaars, S. P.; Mishra, U. K. Electrical Chgaracterization of GaN p-n Junctions with and without Threading Dislocations. *Applied Physics Letters* **1998**, *73*, 975–977.

Nam, O.-H.; Zheleva, T. S.; Bremser, M. D.; Davis, R. F. *Journal of Electronic Materials*, *27*, 233–237.

Paskova, T.; Valcheva, E.; Darakchieva, V.; Paskov, P.; Arnaudov, B.; Monemar, B.; Birch, J.; Heuken, M.; Davis, R. F.; Gibart, P.,: Growth, Separation and Properties of HVPE Grown GaN Films using Different Nucleation Schemes. *Proc. 21st Century COE Joint Workshop on Bulk Nitrides, IPAP Conf. Series* **2002**, *4*, 14–20.

Roskowski, A. M.; Preble, E.; Einfeldt, S.; Miraglia, P. M.; Schuk, J.; Grober, R.; Davis, R. F. Reduction in Dislocation Density and Strain in GaN Thin Films grown via Maskless Pendeo-Epitaxy. *Opto-Electronics Review* **2002**, *10* (4), 261–270.

Yoder, M. Wide Bandgap Semiconductor Materials and Devices. In *IEEE Transactions on Electron Devices* **1996**, *43*, 1633–1636.

Zheleva, T. S.; Nam O.-H.; Ashmawi, W. M.; Griffin, J. D.; Davis, R. F. Lateral Epitaxy and Dislocation Density Reduction in Selectively Grown Heterostructures. *Journal of Crystal Growth* **2001**, *222*, 706–718.

Zheleva, T. S.; Smith, S.; Thomson, D.; Linthicum, K.; Rajagopal, P.; Davis, R. F. Pendeo-Epitaxy – a New Approach for Latteral Growth of Gallium Nitride Films. *Journal of Electronic Materials* **1999**, *28*, L5–L8.

No. Copies	Organization
1	ADMNSTR
PDF	DEFNS TECHL INFO CTR ATTN DTIC OCP (ELECTRONIC COPY) 8725 JOHN J KINGMAN RD STE 0944 FT BELVOIR VA 22060-6218
1	DARPA ATTN IXO S WELBY 3701 N FAIRFAX DR ARLINGTON VA 22203-1714
1	OFC OF THE SECY OF DEFNS ATTN ODDRE (R&AT) THE PENTAGON WASHINGTON DC 20301-3080
1	US ARMY RSRCH DEV AND ENGRG CMND ARMAMENT RSRCH DEV AND ENGRG CTR ARMAMENT ENGRG AND TECHNLGY CTR ATTN AMSRD AAR AEF T J MATTS BLDG 305 ABERDEEN PROVING GROUND MD 21005-5001
1	US ARMY TRADOC BATTLE LAB INTEGRATION & TECHL DIRCTRT ATTN ATCD B 10 WHISTLER LANE FT MONROE VA 23651-5850
1	PM TIMS, PROFILER (MMS-P) AN/TMQ 52 ATTN B GRIFFIES BUILDING 563 FT MONMOUTH NJ 07703
1	US ARMY INFO SYS ENGRG CMND ATTN AMSEL IE TD F JENIA FT HUACHUCA AZ 85613-5300
1	COMMANDER US ARMY RDECOM ATTN AMSRD AMR W C MCCORKLE 5400 FOWLER RD REDSTONE ARSENAL AL 35898-5000
1	US ARMY RSRCH LAB ATTN AMSRD ARL CI OK TP TECHL LIB T LANDFRIED BLDG 4600 ABERDEEN PROVING GROUND MD 21005-5066
1	US GOVERNMENT PRINT OFF DEPOSITORY RECEIVING SECTION ATTN MAIL STOP IDAD J TATE 732 NORTH CAPITOL ST., NW WASHINGTON DC 20402
2	DIRECTOR US ARMY RSRCH LAB ATTN AMSRD ARL RO EV W D BACH ATTN AMSRD AAR AEP F D STEPP PO BOX 12211 RESEARCH TRIANGLE PARK NC 27709-2211
10	US ARMY RSRCH LAB ATTN AMSRD ARL CI OK T TECHL PUB ATTN AMSRD ARL CI OK TL TECHL LIB ATTN AMSRD ARL SE EI U LEE ATTN AMSRD ARL SE RL D EWING ATTN AMSRD ARL SE RL K JONES ATTN AMSRD ARL SE RL M DERENGE ATTN AMSRD ARL SE-RL M ERVIN ATTN AMSRD ARL SE-RL P SHAH ATTN AMSRD ARL SE-RL T ZHELEVA ATTN IMNE ALC IMS MAIL & RECORDS MGMT ADELPHI MD 20783-1197

TOTAL: 22 (1 ELECT, 21 HCS)

INTENTIONALLY LEFT BLANK